A Novel Time-Frequency Analysis for Power System Waveforms Based on "Pseudo-Wavelets"

Cheng Qian, *Graduate Student Member, IEEE*, Mladen Kezunovic, *Fellow, IEEE*

Dept. of Electrical and Computer Engineering
Texas A&M University, College Station
College Station, TX, US
peterqiancheng@tamu.edu, kezunov@ece.tamu.edu

***Abstract*—A novel multiresolution time-frequency analysis method for power system waveforms is proposed. Inspired by wavelet transform, which is widely used in time-frequency analysis of signal to achieve high resolution in both time and frequency domains, the proposed method uses "pseudo-wavelets" and performs similar procedures to calculate the correlations between scaled "pseudo-wavelets" and input signal, revealing the detailed energy distribution of input signal on a wide frequency range throughout the entire data window length. Both mathematical derivation and simulations show that the proposed method is capable of frequency tracking and disturbance detection. By extracting the features of proposed transform on typical power system signals, disturbance classification is also made possible.**

***Index Terms*—Multiresolution analysis, power system disturbance, power system measurements, time-frequency analysis, wavelet transform**

I. INTRODUCTION

Detection and classification of power system waveforms are important topics in power quality studies [1]. Waveforms generated under various operating conditions are characterized by their time-frequency features. Thus, the localization and identification of these features on both time and frequency scales is crucial.

An important branch of signal processing research is the time-frequency analysis. [2] Essentially, time-frequency analysis techniques map the same signal, originally in the form of time-domain waveform samples, onto other domains (spaces). Usually, such mapping or transforms involve tradeoffs between time and frequency resolutions. In time domain analysis, the original acquired signal is decomposed as the superposition of time-domain signals [3], where no frequency information is retained; on the other hand, in frequency domain analysis, Fourier analysis in particular, only the frequency composition is analyzed, which is a major caveat since discontinuities and transients in the data window will not be detected. It is due to Heisenburg uncertainty [4] that time and frequency resolutions cannot be optimized at the same time. Considering the nature of power waveforms where time-frequency fingerprints vary constantly, short-time Fourier transform (STFT) [5] partitions the input signal into smaller analyzing windows by repeatedly applying a sliding time-limited window function, where the frequency analysis of each truncated window is conducted. By doing so, temporal progress is revealed at the expense of sacrificing frequency resolution. Moreover, one of the pitfalls of STFT is invariable time-frequency atom, meaning the selection of such parameters determines the performance of STFT.

Merely a few decades ago, wavelet transform (WT) was invented and has since redefined multiresolution signal processing. [6,7] A mother wavelet, and its scaled and time-shifted versions, termed "children" wavelets, are used as the window functions, and similarities between each child wavelet and input signal are quantified. As a result, the input signal is repeatedly "scanned" by children wavelets with variable time-frequency atom. In WT, the scaling factors of mother wavelet are utilized to signify variations, which are considered a more generalized quantity than frequency. In power system research, WT was used in low frequency electromechanical oscillation detection and analysis [8], and disturbance detection [9]. There are numerous types of mother wavelet families and members, and therefore, the selection of the mother wavelet affects the performance of WT and the interpretation of wavelet coefficients. The features of mother wavelet may be leveraged to analyze certain power signals. For example, Morlet wavelet is proven to be suitable for extracting ringdown patterns [8]. To the authors' best knowledge, there is no mother wavelet "perfectly" designed for all types of signals in the power grid.

Inspired by wavelet analysis, this paper proposes a similar framework for multiresolution time-frequency analysis. The idea is to compare input waveform with a scalable "pseudo-wavelets", such as a single-cycle cosine wave. By analyzing the similarities between scaled "pseudo-wavelets" and input data as time progresses, important features and patterns of the input signal, such as frequency patterns, can be extracted.

This work was supported by the Power Systems Engineering Research Center (PSERC) Project T-57HI "Life-cycle management of mission-critical systems through certification, commissioning, in-service maintenance, remote testing, and risk assessment"

The rest of the paper is organized as follows. The proposed representation using "pseudo-wavelet" is discussed in Section II. Section III considers the implementation issues of the method. Simulations are conducted and results analyzed in Section IV, where the capabilities of proposed method in frequency tracking, disturbance detection and classification are demonstrated. Conclusions and further discussions are given in Section V.

II. Multiresolution Analysis Using "Pseudo-Wavelets"

The mathematical structure of continuous wavelet transform (CWT) is reiterated, and the proposed multiresolution decomposition strategy using "pseudo-wavelets" (PWs) is discussed afterward, followed by the practical interpretation of proposed method.

A. Continuous Wavelet Transform

Mathematically, CWT is defined in (1),

$$\mathbb{CWT}(x,a,b)=\frac{1}{\sqrt{|a|}}\int_{-\infty}^{\infty}x(t)\psi_{a,b}^{*}(\frac{t-b}{a})\mathrm{d}t \qquad (1)$$

where $\psi(t)$ is the mother wavelet function, a is the scaling factor, b is the time-shift factor, and * denotes complex conjugate. Functions $\psi_{a,b}(t) \coloneqq 1/\sqrt{|a|}\,\psi[(t-b)/a]$ are also termed "children wavelets". The wavelets are also time-limited and satisfy $\int\psi_{a,b}(t)\mathrm{d}t\equiv 0$.

Intuitively, CWT calculates the correlations between input signal $x(t)$ and children wavelets $\psi_{a,b}(t)$, with changeable values of a and b. Since the mother and children wavelets are time-limited, the wavelets also serve as windowing that truncates input signal so that only the part of interest is analyzed.

B. Proposed Decompostion with "Pseudo-Wavelet"

Design of wavelets suitable for certain applications is a major research focus in mathematics. In general, using different families/members of mother wavelet in CWT gives distinct results, as shown in Fig. 1. Even though it is evident that energy concentrates in a band and it does not evolve over time, which agrees with the actual signal property, the intensity of energy bands are different and dependent on the choice of wavelet. Besides, scales in the original CWT results need to be translated back to signal properties, for example, frequency, to be meaningful, and this "translation" mechanism relies on wavelet properties and is not always easily found.

In order to acquire a more consistent result, this paper proposed a similar measure for similarity as in (1), but instead of mother wavelet, sinusoidal waves are used. As proven in latter sections, the use of sinusoidal wave is suitable in the background of power system signals, as expressed in (2).

$$\gamma(x;a,b)=\int_{-\infty}^{\infty}\hat{x}(t)\vartheta(\frac{t-b}{a})\mathrm{d}t \qquad (2)$$

where $\gamma(x;a,b)$ denotes the correlation factor between $\hat{x}(t)$ and $\vartheta(t)$ for given a and b, $\hat{x}(t)\coloneqq[x(t)-\bar{x}]/\max[x(t)]$ is the centered and normalized input signal, $\vartheta(t)$ is a customized PW function, and is unit-amplitude cosine wave in this paper. The conjugate in (1) is not used since only real signals are considered.

Analogous to WT, (2) can be interpreted as follows: cosine waves of various frequencies (denoted by a) and time-shifts (denoted by b) are used to repeatedly "scan" the input signal at a multiresolution level. The high frequency components in $\hat{x}(t)$ can be captured by high frequency PW waves, when the envelope varies slow and therefore integrated out; the low frequency components, on the other hand, can be extracted by low frequency PWs, when the fast oscillating components cancel themselves out in the integral. The simplification of WT is legitimate in this case primarily because power signals are predominantly sinusoidal, or superposition of sinusoidal waves. Moreover, it is still possible to detection discontinuities in input signal by applying (2), where the discontinuity manifests changes in signal parameters or system operating conditions.

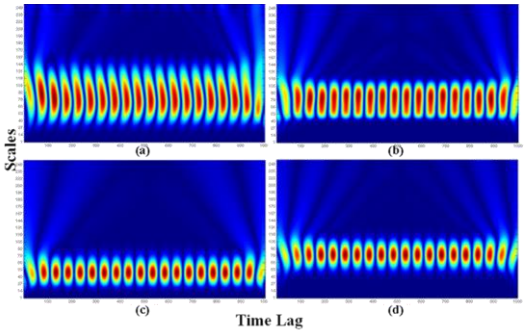

Figure 1. CWT on 60Hz Signal with (a) Daubechies-4 (b) Discrete Meyer (c) Gaussian-4 (d) Morlet wavelets, respectively

C. Extracting Information Using Proposed Decomposition

According to Fourier analysis, an input signal $x(t)$ can be decomposed of the superposition of an infinite number of sinusoidal waves, as shown in (3), known as the inverse Fourier transform:

$$x(t)=\int_{-\infty}^{\infty}X(f)e^{\mathrm{j}2\pi ft}\mathrm{d}f \qquad (3)$$

We may present the proposed method with one of the real components in (3) $x_1(t)$ at frequency $f = f_1$. Consider the correlation integral defined in (2) between $x_1(t)$ and a PW $x_{\mathrm{pw}}(t)$ at frequency $f = f_{\mathrm{pw}}$. Since the PW only has finite support over a span of $T_{\mathrm{pw}} = 1/f_{\mathrm{pw}}$, it is convenient in the derivation that we denote the beginning of PW as time zero. As a result, integral (2) can be simplified as:

$$\gamma(\tau,f_{pw})=\int_{0}^{T_{pw}}x_1(t+\tau)\vartheta(t,f_{pw})\mathrm{d}t \qquad (4)$$

where $x_1(t) = \cos(2\pi f_1 t+\phi_1)$, $\vartheta(t,f_{\mathrm{pw}})\coloneqq \cos(2\pi f_{\mathrm{pw}}t)$, τ denotes the progress along time, or time lag, which only affects the apparent phase angle of $x_1(t)$.

Expand (4) we have:

$$\gamma(\omega_1,\tau)=\int_{0}^{T_{pw}}\cos(\omega_1 t+\omega_1\tau+\phi_1)\cos(\omega_{pw}t)\mathrm{d}t \qquad (5)$$

where $\omega_1 \coloneqq 2\pi f_1$, $\omega_{pw} \coloneqq 2\pi f_{pw}$. To maintain succinct writing, define $\phi_1' \coloneqq \omega_1\tau+\phi_1$. Using trigonometric properties, (5) can be broken down as:

$$\gamma(\omega_1,\phi_1') = \frac{1}{2}\int_0^{T_{pw}} \cos\left[(\omega_1+\omega_{pw})t+\phi_1'\right]\mathrm{d}t + \frac{1}{2}\int_0^{T_{pw}} \cos\left[(\omega_1-\omega_{pw})t+\phi_1'\right]\mathrm{d}t \quad (6)$$

The evaluation of (6) depends on the value ($\omega_1-\omega_{pw}$), and is elaborated as follows:

Case 1: $\omega_1-\omega_{pw}=0$.

$$\gamma(\omega_1,\tau) = \frac{\int_0^{T_{pw}}\cos(2\omega_1 t+\phi_1')\mathrm{d}t + \int_0^{T_{pw}}\cos\phi_1'\mathrm{d}t}{2} = \frac{T_{pw}}{2}\cos\phi_1' = \frac{\pi}{\omega_{pw}}\cos\left(\omega_{pw}\tau+\phi_1\right) \quad (7)$$

The first integral is zero because $2\omega_1 \equiv 2\omega_{pw}$ and the integral on 2nd harmonic over a period is zero.

Case 2: $\omega_1-\omega_{pw}\neq 0$.

$$\gamma(\omega_1,\phi_1') = \frac{\sin\left(\omega_1 T_{pw}+\phi_1'\right)-\sin\phi_1'}{2\left(\omega_1+\omega_{pw}\right)} + \frac{\sin\left(\omega_1 T_{pw}+\phi_1'\right)-\sin\phi_1'}{2\left(\omega_1-\omega_{pw}\right)} \quad (8)$$

$$= \left[\sin\left(\omega_1 T_{pw}+\phi_1'\right)-\sin\phi_1'\right]\frac{\omega_1}{\omega_1^2-\omega_{pw}^2}$$

D. Practical Interpretations of $\gamma(\tau)$

Using L'Hospital's rule, the limit of (8) when $\omega_1 \to \omega_{pw}$ can be evaluated, also note that $\omega_{pw}T_{pw} \equiv 2\pi$:

$$\lim_{\omega_1\to\omega_{pw}}\gamma = \lim_{\omega_1\to\omega_{pw}}\frac{\left[\sin\left(\omega_1\frac{2\pi}{\omega_{pw}}+\phi_1'\right)-\sin\phi_1'\right]\omega_1}{\omega_1^2-\omega_{pw}^2} = \lim_{\omega_1\to\omega_{pw}}\frac{\sin(\omega_1 T_{pw}+\phi_1')+\omega_1 T_{pw}\cos(\omega_1 T_{pw}+\phi_1')-\sin\phi_1'}{2\omega_1} \quad (9)$$

$$= \frac{T_{pw}}{2}\cos\phi_1' = \text{Right-hand side of (7)}$$

Thus, the evaluation of (4) can be expressed by (8), if the value at $\omega_1=\omega_{pw}$ is specified. The zeros of (8) are found by setting $[\sin(\omega_1 T_{pw}+\phi_1')-\sin\phi_1']\cdot\omega_1 = 0$, $\omega_1 \neq \omega_{pw}$:

$$\omega_1 = k\omega_{pw},\ k = 0,2,3,4,\ldots, \text{ or} \quad (10a)$$

$$\omega_1 = \frac{(2k+1)\pi-2\phi_1}{T_{pw}+2\tau},\ k = 0,1,2,3\ldots \quad (10b)$$

According to (10a), when the scanning PW frequency happens to be zero or factors of unknown input power waveform frequency, integral (4) will be zero. For example, when the input waveform is a constant frequency signal at 60Hz, $\gamma(\tau)$ will be showing zero intensity at frequency bands 30Hz, 20Hz, 15Hz, 12Hz, 10Hz, 6Hz, 5Hz, 4Hz, 3Hz, 2Hz, 1Hz, 0Hz (trivial), with sufficient frequency resolution. Equivalently, by identifying the frequency of zero-bands, the actual input waveform frequency can be estimated as the least common multiple of such frequencies.

III. Implementation of Proposed Method

In this section, the proposed method is first implemented by definition given by (4). In order to boost computation efficiency, the proposed method is practically implemented in the matrix form.

A. Preliminary Implementation

In this programming strategy, two FOR-loops are used to enable a scan on both time and frequency using PWs. The pseudo-code is shown in Algorithm 1.

Algorithm 1 Implementation of Proposed Decomposition Method

```
READ input waveform x(t)
DETREND & NORMALIZE input waveform x(t), yielding x̂(t)
DETERMINE frequency axis. Min frequency should be the reciprocal of total data length; max frequency should not exceed Nyquist frequency.
FOR time lag τ, starting from 0 to the end of data window
    CROP x̂(t) according to time lag
    ZERO-PAD so that the data length is the same as x̂(t), yielding x'(t)
    FOR each element of frequency axis
        DETERMINE the values of pseudo-wavelet ϑ(t,f_pw) as a vector
        CROP x'(t) to match the length of pseudo-wavelet
        CALCULATE Hadamard product x'(t)∘ϑ(t,f_pw)
        SAVE result γ(τ,f_pw)
    END
END
```

In reality, the two FOR-loops are extremely inefficient. It is noticeable, however, that the computations inside the FOR-loops are essentially element-wise product (Hadamard product) calculations, which can be expedited by using matrix form.

B. Matrix Formulation of Proposed Method

Algorithm 1 can be considered as an operation repeatedly performed on the same input waveform, but each time some of the old data are deleted, which is analogous to a "hopping" window in STFT. The mechanism is illustrated in Fig. 2.

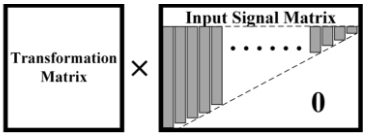

Figure 2. Illustration on the Matrix Formation of Proposed Method

The transformation matrix comprises PWs of a set of pre-defined frequencies, and thus can be generated off-line. The input signal matrix is generated as shown in Algorithm 2, and a simple example is given next to it.

As proved in simulations, utilizing matrix speeds up calculation tremendously, shown in Section IV.C.

IV. Simulation and Analysis

The aforementioned procedures are coded using MATLAB® program. The PC is equipped with Intel® Core® Xeon dual core processor. Sampling frequency is set to be 6 kHz which is close to IED capability. The simulations are performed to test the algorithm's a) capability of tracking

frequencies; b) capability to detect and classify disturbances; and c) computation efficiency of implementation strategies.

Algorithm 2 Generation of Input Signal Matrix (hop size = 1)

1: **READ** input waveform $x(t)$
2: **DETREND & NORMALIZE** input waveform $x(t)$, yielding $\hat{x}(t)$
e.g.: $\hat{x}(t) = [x_1, x_2, x_3]$
3: **FORM** matrix $\hat{A}$=the upper triangle part of $\mathbf{1}_{N\times N}$. $\hat{A}$=`triu(ones(N))`
e.g.: $\hat{A} = \begin{bmatrix} 1 & 1 & 1 \\ 0 & 1 & 1 \\ 0 & 0 & 1 \end{bmatrix}$, N=3
4: **RESHAPE** $\hat{A}$ into column, yielding $\hat{\boldsymbol{a}}_{N^2\times 1}$
e.g.: $\hat{\boldsymbol{a}}$=[1,1,1,0,1,1,0,0,1]^T
5: **FORM** $\hat{\boldsymbol{x}} = [\hat{x}, \hat{x}, \hat{x} \dots, \hat{x}]_{N^2\times 1}$
e.g.: $\hat{\boldsymbol{x}}$=[x_1,x_2,x_3,x_1,x_2,x_3,x_1,x_2,x_3]^T
6: **CALCULATE** Hadamard product $\hat{\boldsymbol{X}}_{N^2\times 1} = \hat{\boldsymbol{x}} \circ \hat{\boldsymbol{a}}$
e.g.: $\hat{\boldsymbol{X}}$=[x_1,x_2,x_3,0,x_2,x_3,0,0,x_3]^T
7: **RESHAPE** $\hat{\boldsymbol{X}}_{N^2\times 1}$ to $\boldsymbol{X}_{N\times N}$
e.g.: $\boldsymbol{X} = \begin{bmatrix} x_1 & 0 & 0 \\ x_2 & x_2 & 0 \\ x_3 & x_3 & x_3 \end{bmatrix}$, when the desired matrix is $\boldsymbol{X}_{\text{input}} = \begin{bmatrix} x_1 & x_2 & x_3 \\ x_2 & x_3 & 0 \\ x_3 & 0 & 0 \end{bmatrix}$
8: **EXTRACT** diagonals of $\boldsymbol{X}_{N\times N}$ using `spdiags`$(\boldsymbol{X}_{N\times N}) \coloneqq (\boldsymbol{X}_2)_{N\times N}$
e.g.: $\boldsymbol{X} = \begin{bmatrix} x_1 & 0 & 0 \\ x_2 & x_2 & 0 \\ x_3 & x_3 & x_3 \end{bmatrix}$, $\boldsymbol{X}_2 = \begin{bmatrix} x_3 & x_2 & x_1 \\ 0 & x_3 & x_2 \\ 0 & 0 & x_3 \end{bmatrix}$
9: **FLIP** in the left-right direction, yielding $\boldsymbol{X}_{\text{input}}$

A. *Frequency Tracking*

As shown in Fig. 3, the intensity of correlation matrix $\boldsymbol{\Gamma}$= $(\gamma)_{ij}$ is depicted as greyness in (a) and contours in (b), and frequencies 10Hz, 12Hz, 15Hz, 20Hz, 30Hz, 60Hz are highlighted with red dashed lines. It can be obviously seen that zero-bands fall into those frequencies. Thereby, (10a) is validated. Besides, by examining the least common multiple of the zero bands of $\boldsymbol{\Gamma}$, the instant frequency can be estimated, although its accuracy is determined by frequency resolution.

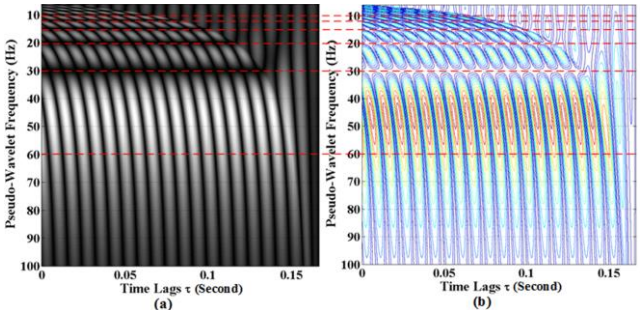

Figure 3. Projection and Contour of Transform Result on 60Hz Waveform

B. *Disturbance Detection and Classification*

The term "disturbance" here is a generic notion referring to any change in the parameters and/or model of input waveforms. Such changes happen regularly in real power system operation and in PMU lab testing. As can be seen in Fig. 4, 0.5s frequency modulation and 0.5s steady state data are concatenated and used as the test signal. Similar to wavelet transform, higher frequency PWs are better at detecting disturbances, as it can be easily seen that before τ=0.5s, the input waveform is frequency-modulated; and after τ=0.5s, it appear to be in steady state.

In practice, it is usually not necessary to extract all frequency components. The "zero-bands" on the contour are especially significant since they reveal frequency trajectories, which are indicative of current operating conditions. Shown in Fig. 5 are the typical responses from typical PMU test waveforms. [10] In each test case, a 0.5 second (30 cycles) waveform is generated, where the last ¼ of the waveform returns to 60Hz steady state (referred to as the "reference condition").

Under steady state test waveforms, shown in Fig. 5(a) 65Hz input, and Fig. 5(b) 5th harmonic input, it can be seen that the factors of instant frequencies (marked by the horizontal zero-bands) remain stable. In Fig. 5(a), the zero-bands are shifted compared to reference waveform, as discussed in Fig. 3; in Fig. 5(b), it is evident that more frequency component are presented than reference condition.

On the other hand, under dynamic state waveforms, the frequency components and/or frequency trajectories change throughout time. Since in power systems, such transients are rather slow compared to data window size, revelation of spectrum details depends heavily on frequency resolution. Regardless, 0.1Hz is adequate to provide an insight of the signal. Each type of input test waveform is characterized by distribution of energy on difference frequencies, which is revealed in the contours. For examples, amplitude-modulated waveform Fig. 5(c) features oscillation of signal energy near nominal frequency; frequency-modulated waveforms Fig. 5(d) shows oscillation of all frequency components; in frequency ramping waveforms Fig. 5(e) and (f), the zero-bands move slowly based on the sign of ramp. It is shown that the PW method can be used to classify power waveforms.

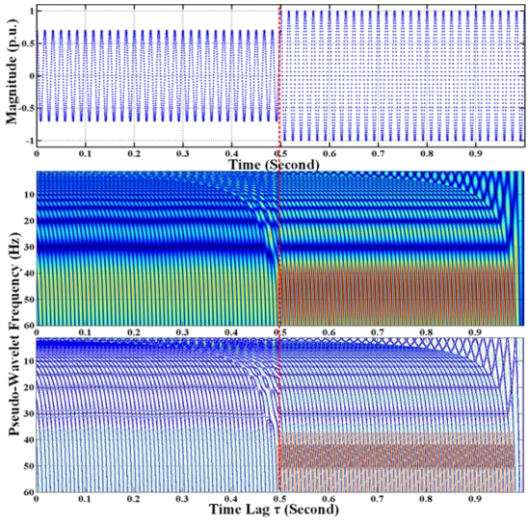

Figure 4. DTFT and DFT of Rectangular Window

It is also worth noting that despite the illustrations given in the paper, in reality, to achieve faster response, tracking the zero-bands is done through computer programming, as depicting a contour figure is very time-consuming, and the human eyes may not be able to detect the changes.

C. *Computation Efficiency Analysis*

In this simulation, the justification of matrix formulation is provided by comparing the computation time of matrix implementation with Algorithm 1. Input data array size (therefore considering sampling rate and data window length),

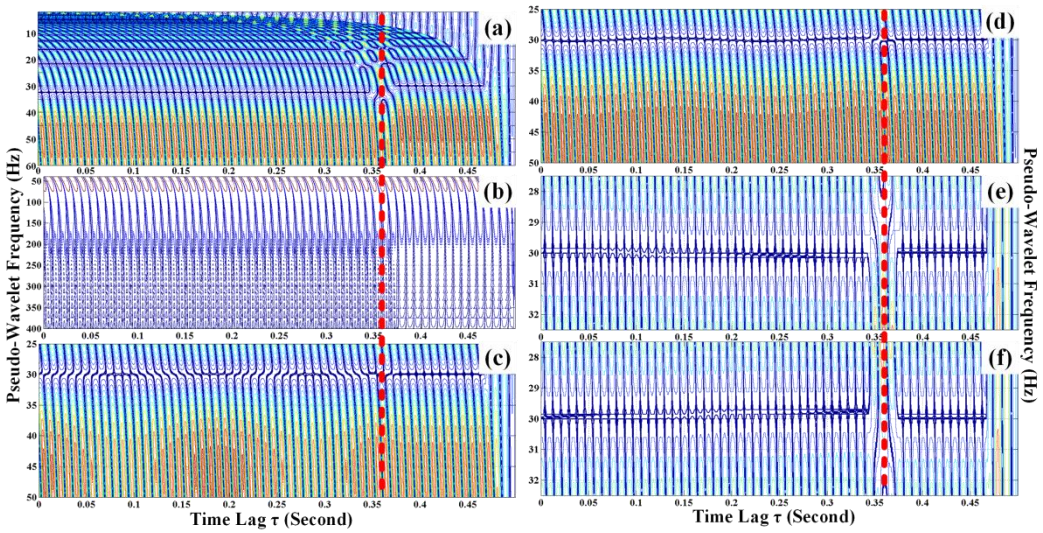

Figure 5. PWT Result for Multiple Test Waveforms: (a) Static 65Hz; (b) 5th Harmonic; (c) Amplitude Modulation; (d) Frequency Modulation; (e) Frequency Ramping at 1Hz/s; (f) Frequency Ramping at -1Hz/s

frequency range (max and min frequency and frequency resolution) are considered as the contributing factors.

Computation times as well as the memory allocations are also displayed. Only 4 cases are tested since they already provide very evident and consistent results, shown in Table I.

TABLE I. COMPUTATION EFFICIENCY TEST OF TWO IMPLEMENTATION STRATEGIES

Case Details	**Matrix Γ Size (Time, Freq.)**	**Computation Time**	
		Matrix Formulation	***Two FOR-loops***
10 cycles, f_{sam}=6kHz 6Hz~60Hz, REZ 0.1Hz	(1000,541) 4.324MB	0.069s	9.667s
10 cycles, f_{sam}=6kHz 6Hz~120Hz, REZ 0.1Hz	(1000,1141) 9.128MB	0.073s	17.115s
20 cycles, f_{sam}=6kHz 3Hz~120Hz, REZ 0.1Hz	(2000,1171) 18.736MB	0.250s	37.117s
30 cycles, f_{sam}=6kHz 2Hz~60Hz, REZ 0.01Hz	(3000,5801) 139.224MB	0.596s	356s

Note: REZ: resolution; Freq.: frequency

V. CONCLUSION AND FURTHER DISCUSSIONS

This paper presents a novel approach to extract power system frequency features which can be thereafter employed for disturbance classification and identification. The contributions are:

- The concept of using other types of scalable signals (termed "pseudo-wavelets" in the paper) is promoted. The PWs should be structured to fit power system application in order to extract feature of interest. The proposed concept aims to serve as a simplification of WT in power system to provide more concise waveform analysis.
- Cosine waves are used in this paper to address the concept. Mathematical expressions of proposed method are derived and discussed.
- The proposed method is capable of frequency tracking, disturbance detection and classification. As shown in simulations, proposed method can reveal the frequency details in typical power system test waveforms defined in [10], and thereafter facilitate the classification and identification of input test waveforms.
- The original iteration-dependent algorithm can be easily optimized into matrix calculation, which enables fast calculation and therefore has practical significance.

REFERENCES

[1]. A. M. Gaouda, M. M. A. Salama, M. R. Sultan and A. Y. Chikhani, "Power quality detection and classification using wavelet-multiresolution signal decomposition," in IEEE Transactions on Power Delivery, vol. 14, no. 4, pp. 1469-1476, Oct 1999.

[2]. A. N. Akansu, R. A. Haddad, "Multiresolution Signal Decomposition, Transform, Subbands, and Wavelets (Second Edition)," Academic Press, 2001, pp.331-390.

[3]. C. Qian, T. Bi, J. Li, H. Liu and Z. Liu, "Synchrophasor estimation algorithm using Legendre polynomials," 2014 IEEE PES General Meeting | Conference & Exposition, National Harbor, MD, 2014, pp. 1-5.

[4]. A. Agaskar and Y. M. Lu, "A Spectral Graph Uncertainty Principle," in IEEE Transactions on Information Theory, vol. 59, no. 7, pp. 4338-4356, July 2013.

[5]. Y. H. Gu and M. H. J. Bollen, "Time-frequency and time-scale domain analysis of voltage disturbances," in IEEE Transactions on Power Delivery, vol. 15, no. 4, pp. 1279-1284, Oct 2000.

[6]. I. Daubechies, "The wavelet transform, time-frequency localization and signal analysis," in IEEE Transactions on Information Theory, vol. 36, no. 5, pp. 961-1005, Sep 1990.

[7]. G. Strang, T. Nguyen, "Wavelets and Filter Banks," Wellesley-Cambridge Press, 1997, pp. 220-262.

[8]. J. L. Rueda, C. A. Juarez and I. Erlich, "Wavelet-Based Analysis of Power System Low-Frequency Electromechanical Oscillations," in IEEE Transactions on Power Systems, vol. 26, no. 3, pp. 1733-1743, Aug. 2011.

[9]. J. Ren and M. Kezunovic, "An Adaptive Phasor Estimator for Power System Waveforms Containing Transients," in IEEE Transactions on Power Delivery, vol. 27, no. 2, pp. 735-745, April 2012.

[10]. IEEE Standard for Synchrophasor Measurements for Power Systems -- Amendment 1: Modification of Selected Performance Requirements," in IEEE Std C37.118.1a-2014 (Amendment to IEEE Std C37.118.1-2011), vol., no., pp.1-25, April 30 2014.